Copper/Graphene/Clay Nanohybrid: A Highly Efficient Heterogeneous Nanocatalyst for the Synthesis of Novel 1,2,3-Triazolyl Carboacyclic Nucleosides *via* 'Click' *Huisgen* 1,3-Dipolar Cycloaddition

by **Mohammad Navid Soltani Rad***[a], **Somayeh Behrouz***[a], **S. Jafar Hoseini**[b], **Hasan Nasrabadi**[b], and **Maryam Saberi Zare**[a]

[a]) Medicinal Chemistry Research Laboratory, Department of Chemistry, Shiraz University of Technology, Shiraz 71555-313, Iran (phone: +98-71-37261392; fax: +98-71-37354523; e-mail: soltani@sutech.ac.ir, behrouz@sutech.ac.ir)

[b]) Department of Chemistry, Faculty of Sciences, Yasouj University, Yasouj 7591874831, Iran

A very mild and highly efficient synthesis of some novel 1*H*-1,2,3-triazolyl carboacyclic nucleosides *via* a 'Click' *Huisgen* cycloaddition of *N*-propargyl nucleobases and azido alcohols using Cu/aminoclay/reduced graphene oxide nanohybrid (Cu/AC/r-GO nanohybrid) as nanocatalyst is described. The preparation and characterization of Cu/AC/r-GO nanohybrid are discussed. This catalyst was characterized by X-ray diffraction, FT-IR, TEM, and energy-dispersive analysis of X-ray techniques. Cu/AC/r-GO nanohybrid is a stable and highly efficient heterogeneous nanocatalyst that can be easily prepared, used, and restored from the reaction mixture by simple filtration, and reused for many consecutive trials without significant decrease in activity.

Introduction. – Drug design and synthesis based on non-natural nucleosides are prominence strategies to overcome miscellaneous infections and diseases caused by viruses, bacteria, cancer, *etc.* [1]. Three main strategies are normally applied on natural nucleosides to access a great deal of diverse non-natural nucleosides, encompassing *i*) modification of functionalities on nucleobases and/or replacement of nucleobases with their similar heterocyclic analogs or isosteres; *ii*) alteration of the sugar residue's backbone, and finally *iii*) conversion, as well as conjugation of free OH groups to various functionalities [2]. In connection with the first strategy, it is well demonstrated and fully established that the replacement of purine and pyrimidine nucleobases in natural nucleosides with those of azole derivatives not only doesn't abolish the biological activity, but also endows the leading properties [3]. This inspiration in nucleobase change has been emerged in the design and synthesis of well-established non-natural nucleosides, *i.e.*, ribavirin (virazole), mizoribine (bredinin), pyrazofurine, and *tert*-butyldimethylsilylspiroaminooxathioledioxide (TSAO), which exhibit antiviral, antitumor, and immunosuppressive activities (*Fig. 1*) [4].

Since the discovery of zidovudine (AZT; *Fig. 1*) as potent anti-HIV drug [5], enormous efforts were conducted to conjugate the AZT scaffold with various naturally occurring molecules or drugs [6]. In this regard, the *Huisgen* azide–alkyne cycloaddition was found to be a highly efficient and reliable tool for tethering AZT to diverse molecules [6]. This became the starting point for extensive endeavors to incorporate 1*H*-1,2,3-triazolyl cores into the nucleoside framework [7]. In general, the

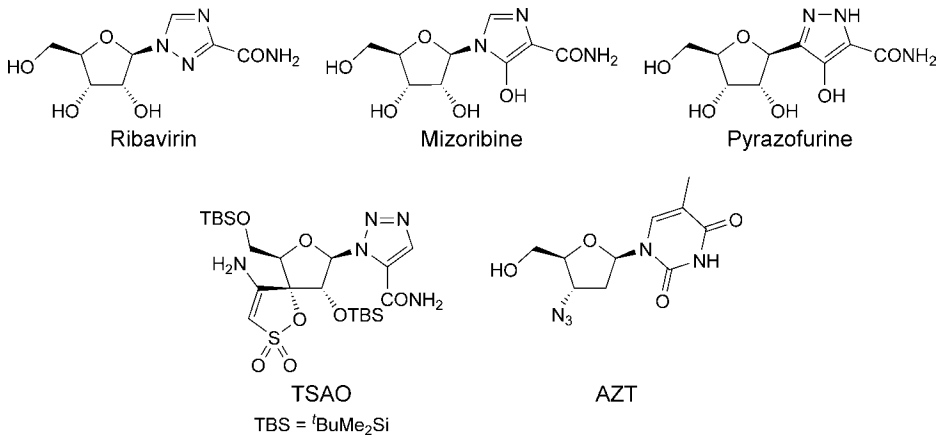

Fig. 1. *Structures of some famous non-natural nucleosides*

incorporation of the 1*H*-1,2,3-triazolyl group into a molecular scaffold is an interesting task, since the 1*H*-1,2,3-triazolyl moiety involves remarkable biological activities, as well as recognition by enzymes and receptors in the cell [8]. Moreover, 1*H*-1,2,3-triazolyl cores are known as the non-classical isostere of amide because of having considerable topological and electronic similarities. Given the biological importance of 1*H*-1,2,3-triazolyl cores, they have been extensively used in the design of new nucleosides as surrogate moieties in different fragments of the nucleosides, comprising *i*) a nucleobase surrogate; *ii*) a single substituent linked to sugar or nucleobase residues; *iii*) a splicer between nucleoside (from sugar or nucleobase sites) and other biomolecules to access nucleoside–nucleoside, nucleoside–drug conjugates, *etc.*; and *iv*) a spacer between nucleobase and sugar or sugar mimic moieties. Among the aforementioned 1,2,3-triazolyl-nucleoside analogs, the fourth status has recently received extensive attention because of their noticeable biological activities like antiviral, antitumor, and antimicrobial activities, and binding affinity to enzymes [9].

Huisgen's Cu^{I}-catalyzed azide–alkyne cycloaddition (CuAAC) has emerged as a powerful tool for introducing the 1*H*-1,2,3-triazolyl residue into a molecular structure [10]. Active Cu^{I} as the catalytic species plays a crucial role in the regioselectivity of the *Huisgen* cycloaddition, providing only 1,4-disubstituted isomers. Active Cu^{I} can be prepared in miscellaneous ways, encompassing *in situ* reduction of Cu^{II} salts mostly in the presence of vitamin C [11], oxidation of Cu^{0} [12], and/or Cu^{II}/Cu^{0} comproportionation [13]. Due to several drawbacks by the use of Cu^{I} salts, especially the formation of undesired alkyne–alkyne homocoupling side products, their application in simple form was limited [14]. To overcome this problem, active Cu^{I} is complexed to N- or P-based ligands, or immobilized on various solid supports [15]. Different solid materials were used to support the Cu species, comprising silica gel, zeolites, alumina, charcoal, montmorillonite, amine-functionalized silica or polymer, *etc.* [16]. Among the solid supports, those with covalently bonded amine residues are more satisfactory because of their capability to chelate with the Cu species [17]. This chelation not only causes an enhancement of Cu^{I}-catalytic activity, but also largely prevents desorption of the Cu

species from the surface of the support, whilst simple surface absorption of Cu species on the surface of a raw support is accompanied with major leaching during the course of reaction. This current drawback extensively diminishes the reusability and recoverability of the catalyst.

Graphene oxide (GO) as synthetic precursor of graphene is a unique substance that can be regarded as a single monomolecular layer of graphite with various O-bearing functionalities such as OH, C=O, COOH, and epoxide groups [18]. The presence of theses functionalities allows grafting of GO with many biomolecules, organic materials, drugs, *etc.*, that found extensive applications in electronics, energy storage, biomedical applications (drug delivery), and biosensors [19]. After functionalizing or modifying GO with desired molecules, the modified GO is reduced to graphene (r-GO) to retrieve the exclusive mechanical, electrical, thermal, and optical properties known from graphene [20].

In continuation of our ongoing research on the preparation of heterogeneous nano-Cu catalysts and their application in organic transformation [16][21], hereby, we have explained the preparation and characterization of Cu/aminoclay/reduced graphene oxide nanohybrid (Cu/AC/r-GO nanohybrid) as highly efficient novel nanohybrid catalyst for the very mild synthesis of some 1*H*-1,2,3-triazolyl carboacyclic nucleosides *via* a 'Click' *Huisgen* cycloaddition of *N*-propargyl nucleobases and azido alcohols in THF/H_2O at room temperature (*Scheme*).

Results and Discussion. – The powder X-ray diffraction pattern of the Cu/AC/r-GO nanohybrid obtained by precipitation from freshly prepared aqueous Cu/AC/r-GO suspension (*Fig. 2*) shows peaks corresponding to (111), (200), and (220) planes associated with the fcc structure of Cu. The observation of low-angle peaks corresponding to the interlayer spacing of AC suggest the possible coexistence of staked nanostructures made up of few layers of AC. AC/GO hybrid has been converted to AC/r-GO hybrid by reduction *via* $N_2H_4 \cdot H_2O$. r-GO shows a diffraction peak for C(002) at $2\theta = 27°$ similar to that of carbon black [22].

The Cu/AC/r-GO nanohybrid was further examined by an energy-dispersive analysis of X-ray (EDAX) where Cu, Mg, Si, and O along with carbon elements, which could be attributed to the synthesis of the Cu/AC/r-GO nanohybrid, were observed (*Fig. 3*).

For TEM, the aqueous Cu/AC/r-GO suspension was first precipitated by the addition of excess EtOH and then re-dispersed in EtOH by sonication before drop casting on a carbon-coated Cu grid. The TEM images show the presence of clay nanoparticles ranging from 10 to 70 nm in size distributed on the r-GO sheet (*Fig. 4, a* and *b*). Also, the TEM image of a freshly prepared sample shows Cu particles of less than 15 nm in size on the backdrop of the AC/r-GO hybrid (*Fig. 4, c*).

The IR spectrum of the Cu/AC/r-GO nanohybrid clearly indicated the formation of the catalyst. As shown in *Fig. 5*, the peaks at 2854 and 2925 cm^{-1} correspond to symmetric *vs.* CH_2 and asymmetric *vs.* CH_2 of the alkyl chains, respectively, which are assigned to aminoclay. Moreover, the bands at 1116 (Si–C) and 1034 cm^{-1} (Si–O–Si) provide more evidence for the presence of aminoclay [23]. The IR spectrum also shows bands at 3405, 1731, 1621, and 1216 cm^{-1}, indicating that r-GO sheets are present as the prepared hybrid [24].

Scheme. *Synthesis of Novel 1*H-*1,2,3-Triazolyl Carboacyclic Nucleosides* via *the 'Click'* Huisgen *Cycloaddition Using the Cu/AC/r-GO Nanohybrid*

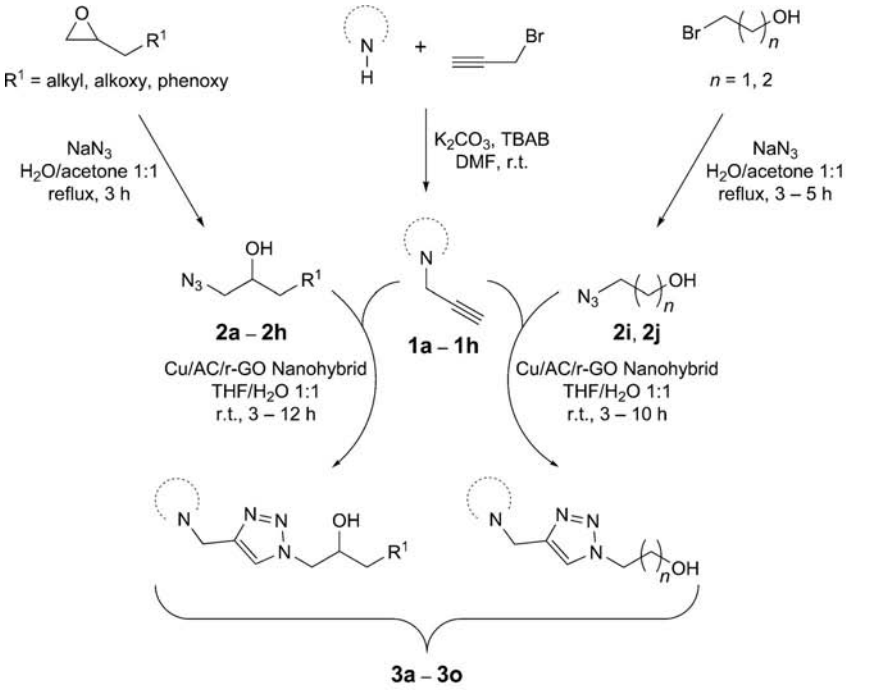

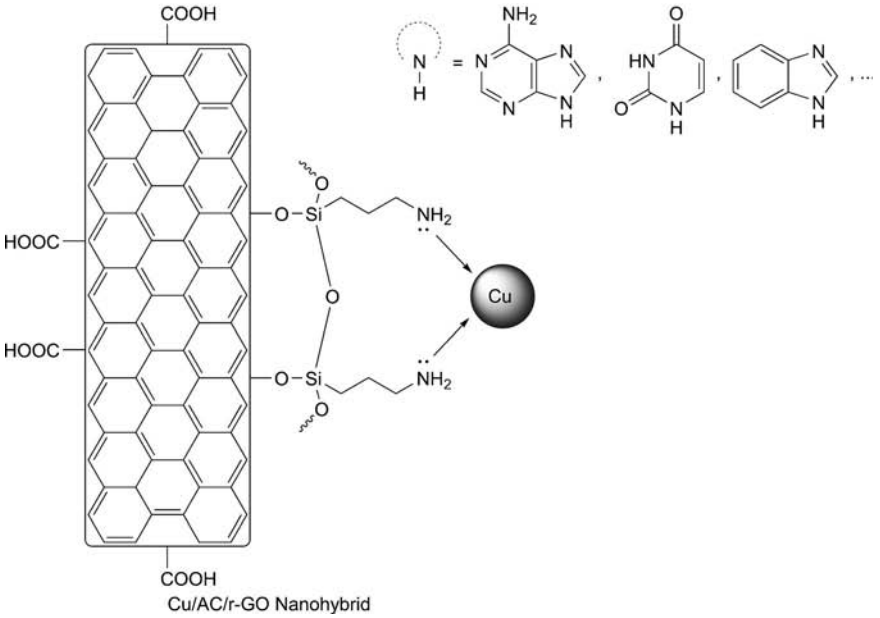

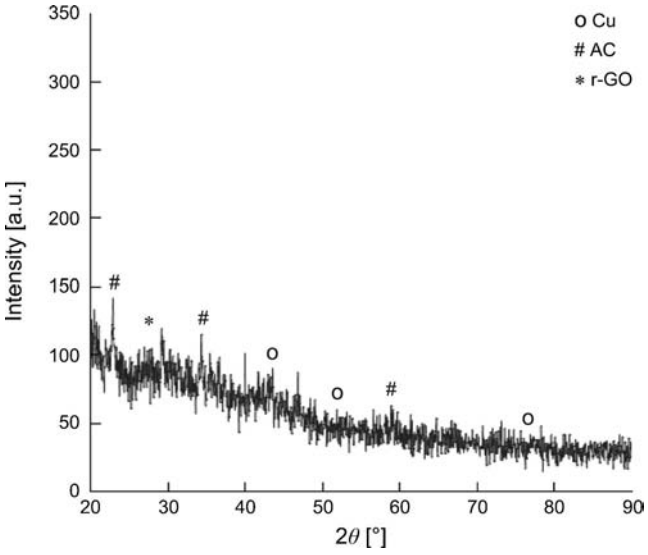

Fig. 2. *XRD Pattern of the Cu/AC/r-GO nanohybrid*

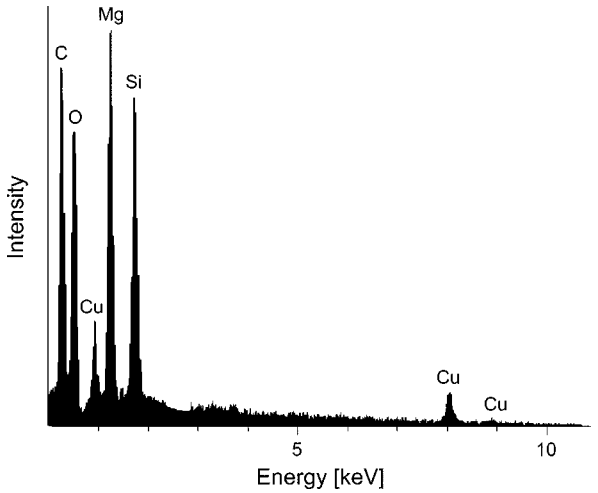

Fig. 3. *EDAX Spectrum of the Cu/AC/r-GO nanohybrid*

Having prepared the Cu/AC/r-GO nanohybrid, we initiated the synthesis of 1*H*-1,2,3-triazolyl carboacyclic nucleosides by selective *N*-propargylation of nucleobases and other N-heterocyclic compounds, **1a**–**1h**. Due to the ambident nature of nucleobases, *N*-alkylation should be conducted regioselectively under mild reaction conditions. In this context, among the established methods so far, a mild method reported by *Lazrek* and co-workers [25] has shown better selectivity and efficiency. In this method, *N*-propargylation of nucleobases is achieved in the presence of K_2CO_3 in

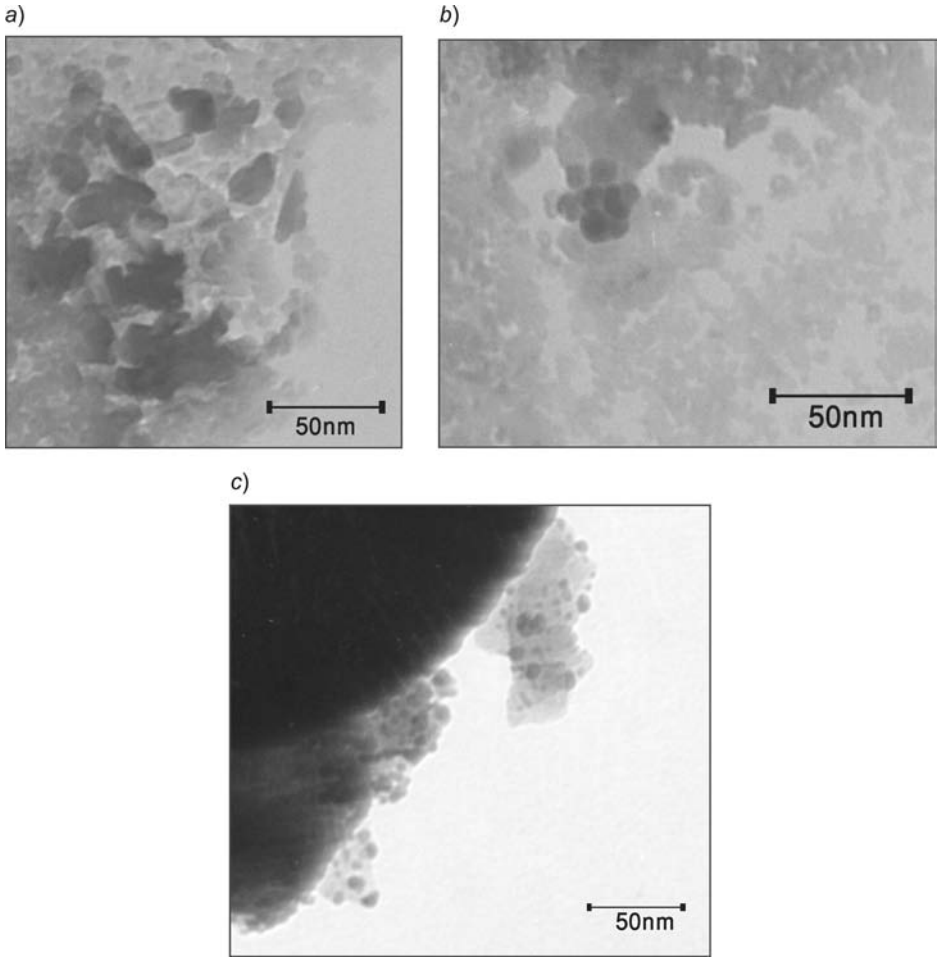

Fig. 4. *TEM Images of the Cu/AC/r-GO nanohybrid. a*), *b*) Clay nanoparticles (10–70 nm in size) distributed on the r-GO sheet. *c*) Cu particles (less than 15 nm in size) on the backup of the AC/r-GO hybrid.

DMF at ambient temperature. To our experience, addition of a catalytic amount of Bu_4NBr (TBAB) can largely enhance the efficiency and shorten the reaction time while retaining the regioselectivity trend. Thus, the desired alkynes, N^1-propargyluracils **1a** and **1b**, N^9-propargyladenine (**1c**), N^7-propargyltheophylline (**1d**), N^1-propargyltheobromine (**1e**), N^1-propargylbenzimidazoles **1f** and **1g**, and N^1-propargyl-2-methyl-4-nitroimidazole (**1h**) were obtained in good to excellent yields.

After the preparation of alkynes **1a**–**1h**, azido alcohols were prepared in the next step. Azido alcohols in the preparation of 1*H*-1,2,3-triazolyl carboacyclic nucleosides have an apparent privilege compared with simple alkyl azide analogs, since the application of azido alcohols introduces a OH group as a crucial site for potential phosphorylation *via* phosphate kinases in the cell [26]. In this regard, two different

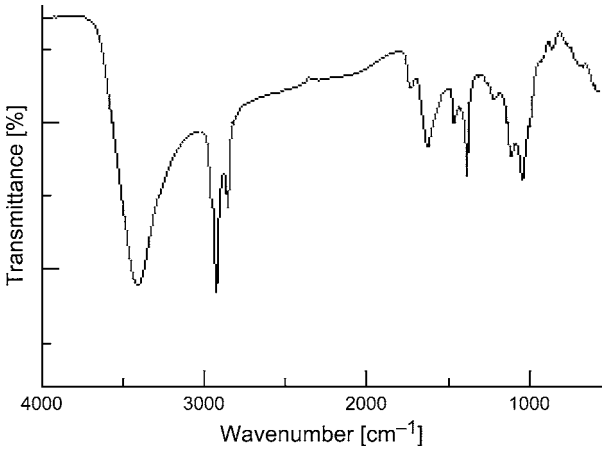

Fig. 5. *FT-IR Spectrum of the Cu/AC/r-GO nanohybrid*

types of azido alcohols, including branched and unbranched (linear) structures, were prepared for 'Click' *Huisgen* cycloaddition with **1a**–**1h**. Branched azido alcohols **2a**–**2h** were prepared by regioselective ring opening of epoxides *via* N_3^- in acetone/H_2O solution under reflux, whereas unbranched azido alcohols **2i** and **2j** were prepared from 2-bromoethanol and 3-bromopropan-1-ol, respectively, under similar conditions and almost in quantitative yields.

To find the optimized reaction conditions, the cycloaddition of **1a** with **2d** was designated as a sample reaction and the influence of factors like solvent and catalyst was investigated.

Due to the polar nature of the 'Click' *Huisgen* cycloaddition, the solvent plays a critical role in this reaction. To our experience [16][21], the combination of H_2O with H_2O-miscible organic solvents often progresses the reaction satisfactorily. As can be seen in *Table 1*, a 1:1 mixture of organic solvents in H_2O was tested for cycloaddition of **1a** and **2d** in the presence of a catalytic amount of Cu/AC/r-GO nanohybrid at room temperature. The most appropriate result was obtained when a THF/H_2O mixture was applied (*Table 1*, *Entry 8*). However, other mixtures also afforded moderate to good yields of **3d** after longer times (*Table 1*, *Entries 1–7*). When H_2O was used alone, the low yield of **3d** was attained after a much longer time. The low yield obtained for **3d** using pure H_2O, is attributed to a lack of solubility of the starting materials in H_2O under the examined conditions.

Inductively coupled plasma (ICP) analysis indicated that in each gram of catalyst, there are 0.013 g of active Cu catalyst (0.02 mol-%). To determine the optimized amount of Cu/AC/r-GO nanohybrid, different amounts of catalyst were examined in the model reaction (*Table 2*). As depicted in *Table 2*, the best result was obtained when 0.008 or 0.010 mol-% of catalyst were applied (*Table 2*, *Entries 4* and *5*). The use of an excess amount of catalyst has a negligible effect on the progress of the reaction. To investigate the catalytic potency of Cu/AC/r-GO nanohybrid in the synthesis of 1*H*-1,2,3-triazolyl carboacyclic nucleosides, we tested the model reaction using other Cu catalysts and compared the results with that of Cu/AC/r-GO nanohybrid (*Table 3*).

Table 1. *Influence of H_2O Mixture with Some H_2O-Miscible Organic Solvents on Cycloaddition of* **1a** *with* **2d** *Using Cu/AC/r-GO Nanohybrid at Room Temperature*[a])

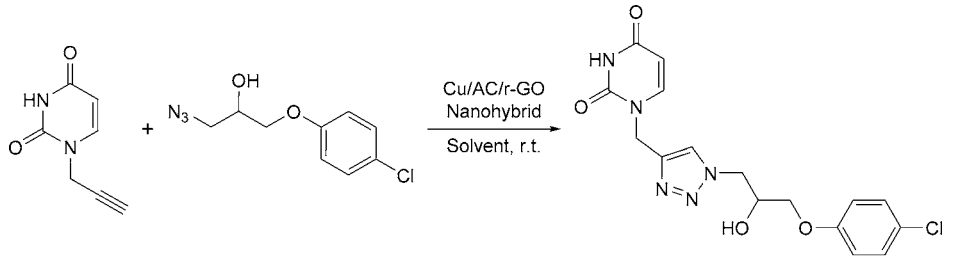

1a **2d** **3d**

Entry	Solvent[b])	Time [h]	Yield [%][c])
1	H_2O/MeCN	10	68
2	H_2O/DMF	8	77
3	H_2O/DMSO	7	70
4	H_2O/EtOH	10	58
5	H_2O/acetone	8	66
6	H_2O/dioxane	6	75
7	H_2O/HMPA[d])	9	61
8	H_2O/THF	5	84
9	H_2O	12	53

[a]) Reagents and conditions: **1a** (0.01 mol), **2d** (0.012 mol), Cu/AC/r-GO nanohybrid (0.008 mol-%), solvent (30 ml), room temperature. [b]) A 1 : 1 mixture of solvents was used. [c]) Yield of isolated product. [d]) HMPA, hexamethylphosphoramide.

Table 3 shows that despite favorable activities assessed for different examined Cu salts (Cu^I or Cu^{II}), however, the most satisfactory result was observed when the Cu/AC/r-GO nanohybrid was applied. The improved performance of the Cu/AC/r-GO nanohybrid in comparison with other Cu catalysts is rationalized to potential $\pi\cdots\pi^*$ interaction of electron-enriched r-GO as a polynuclear aromatic sheet with electron-deficient nucleobases [27].

To determine the scope of the Cu/AC/r-GO nanohybrid in the synthesis of other 1*H*-1,2,3-triazolyl carboacyclic nucleosides, the optimized conditions were screened to other *N*-propargylated nucleobases, **1a**–**1h**, and azido alcohols **2a**–**2j** (*Table 4*). As depicted in *Table 4*, diverse *N*-propargylated nucleobases, comprising purines, pyrimidines, and azoles with branched or unbranched azido alcohols, were regioselectively and efficiently converted to their corresponding 1,4-disubstituted triazolyl carboacyclic adducts by the 'Click' *Huisgen*'s cycloaddition using the Cu/AC/r-GO nanohybrid in excellent yields under very mild conditions. Compounds **3a**–**3o** were fully characterized, and their structures were confirmed by physical and spectroscopic techniques including IR, ^{1}H- and ^{13}C-NMR, MS, and elemental analysis. In general, the presence of a *singlet* at δ(H) 7.50–8.20 in the ^{1}H-NMR spectra is a main criterion for a H-atom at C(5) of the 1*H*-1,2,3-triazole moiety in all synthesized triazolyl carboacyclic nucleosides.

Table 2. *Influence of Catalyst Amount on Cycloaddition of* **1a** *with* **2d** *Using Cu/AC/r-GO Nanohybrid at Room Temperature*[a])

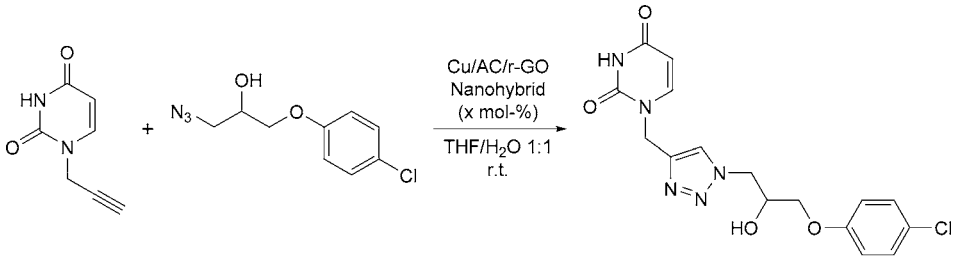

1a **2d** **3d**

Entry	Cu/AC/r-GO Nanohybrid [mol-%]	Time [h]	Yield [%][b])
1	0.002	11	58
2	0.004	9	64
3	0.006	8	68
4	0.008	5	84
5	0.010	5	84
6	0.012	6	81
7	0.014	7	80
8	0.016	7	80

[a]) Reagents and conditions: **1a** (0.01 mol), **2d** (0.012 mol), Cu/AC/r-GO nanohybrid (*x* mol-%), THF/H_2O 1 : 1 (30 ml), room temperature. [b]) Yield of isolated product.

Table 3. *Comparison of Various Cu Catalysts with Cu/AC/r-GO Nanohybrid on Cycloaddition of* **1a** *with* **2d** *at Room Temperature*[a])

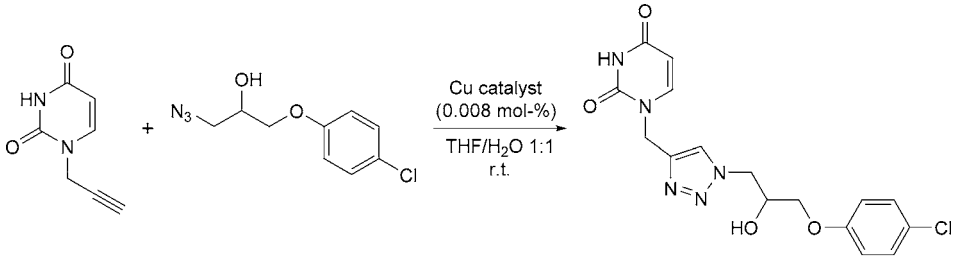

1a **2d** **3d**

Entry	Cu Catalyst	Time [h]	Yield [%][b])
1	Cu/AC/r-GO Nanohybrid	5	84
2	Cu_2O	9	67
3	CuI	5	78
4	$Cu(acac)_2$[c])	11	59
5	$CuSO_4 \cdot 5\ H_2O$[c])	8	68
6	$(AcO)_2Cu$[c])	8	63
7	$Cu(OTf)_2$[c])	7	70

[a]) Reagents and conditions: **1a** (0.01 mol), **2d** (0.012 mol), Cu catalyst (0.008 mol-%), THF/H_2O 1 : 1 (30 ml), room temperature. [b]) Yield of isolated product. [c]) The reaction was carried out in the presence of sodium ascorbate (0.1 mol-%).

Table 4. *Cu/AC/r-GO Nanohybrid-Catalyzed Synthesis of 1*H*-1,2,3-Triazolyl Carboacyclic Nucleosides*[a])

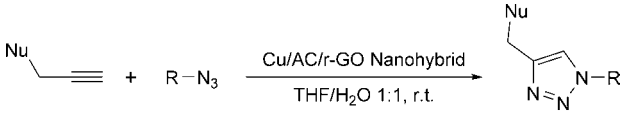

1a – 1h **2a – 2j** **3a – 3o**

Entry	Alkyne (Nu)	Azido alcohol (R)	Product[b])	Time [h]	Yield [%][c])
1	*N*[1]-Uracilyl	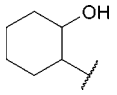	**3a**	7	88
2	*N*[1]-uracilyl	$Me(CH_2)_5CH(OH)CH_2$	**3b**	8	92
3	*N*[1]-uracilyl	$MeCH_2CH(OH)CH_2$	**3c**	7	90
4	*N*[1]-uracilyl	4-Cl–C_6H_4–$OCH_2CH(OH)CH_2$	**3d**	5	84
5	*N*[1]-6-azauracilyl	2,4-Cl_2–C_6H_3–$OCH_2CH(OH)CH_2$	**3e**	4	81
6	*N*[7]-theophyllinyl	4-Me–C_6H_4–$OCH_2CH(OH)CH_2$	**3f**	3	93
7	*N*[7]-theophyllinyl	4-MeO–C_6H_4–$OCH_2CH(OH)CH_2$	**3g**	3	90
8	*N*[7]-theophyllinyl	$HO(CH_2)_2$	**3h**	4	94
9	*N*[1]-theobrominyl	$HO(CH_2)_2$	**3i**	8	80
10	*N*[9]-adeninyl	$HO(CH_2)_2$	**3j**	10	82
11	*N*[9]-adeninyl	$HO(CH_2)_3$	**3k**	10	85
12	*N*-benzimidazolyl	$HO(CH_2)_2$	**3l**	9	86
13	*N*-benzimidazolyl	$PhOCH_2CH(OH)CH_2$	**3m**	12	80
14	*N*-2-methylbenzimidazolyl	$HO(CH_2)_2$	**3n**	8	87
15	*N*[1]-2-methyl-4-nitroimidazolyl	$HO(CH_2)_3$	**3o**	10	91

[a]) Reagents and conditions: **1a** (0.01 mol), **2d** (0.012 mol), Cu catalyst (0.008 mol-%), THF/H_2O 1:1 (30 ml), room temperature. [b]) All products were characterized by IR, ^{1}H- and ^{13}C-NMR, MS, and elemental analysis. [c]) Yield of isolated product.

The reusability and recoverability of the Cu/AC/r-GO nanohybrid in the sample reaction was also evaluated. In this regard, before using and also final testing of the catalyst for its activity in many successive runs, the catalyst was recycled from the reaction mixture through a sintered glass funnel by vacuum-filtering. Afterwards, the catalyst was washed successively with anhydrous THF or acetone (10 ml) and dried in a vacuum oven at 80° for 1 h. The catalyst was tested in five consecutive runs, and no fresh catalyst was added. As can be seen in *Table 5*, the Cu/AC/r-GO nanohybrid can be recycled and reused for many consecutive trials without significant loss of activity. Furthermore, the ICP analysis has confirmed the reusability of the Cu/AC/r-GO nanohybrid without significant desorption of Cu species from AC/r-GO matrix. As it is well indicated, the amount of leached Cu from Cu/AC/r-GO nanohybrid is extremely negligible (0.008% after five consecutive runs), and it is rationalized due to a powerful binding present between the Cu species and AC group on the surface of r-GO.

In summary, the fabrication and characterization of a novel Cu/AC/r-GO nanohybrid as a highly efficient heterogeneous nanocatalyst in the synthesis of some 1,2,3-triazolyl carboacyclic nucleosides has been discussed. The Cu/AC/r-GO nanohybrid

Table 5. *Reusability of Cu/AC/r-GO Nanohybrid in Successive Runs for the Synthesis of* **3d**[a])

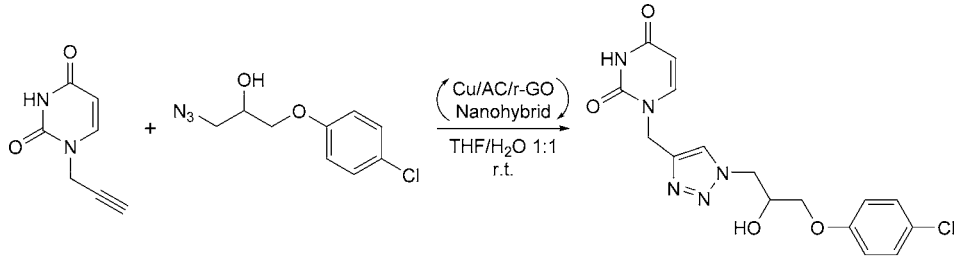

1a **2d** **3d**

Run	Time [h]	Yield [%][b])
1	5	84
2	5	84
3	6	82
4	7	81
5	7	80

[a]) Reagents and conditions: **1a** (0.01 mol), **2d** (0.012 mol), Cu catalyst (0.008 mol-%), THF/H_2O 1:1 (30 ml), room temperature. [b]) Yield of isolated product.

was efficiently utilized in the mild synthesis of 1,4-disubstituted 1*H*-1,2,3-triazolyl carboacyclic nucleosides through regioselective 'Click' *Huisgen* cycloaddition of *N*-propargylated nucleobases and azido alcohols in H_2O/THF 1:1 at room temperature, and the products were obtained in excellent yields. The Cu/AC/r-GO nanohybrid was shown to be a chemically and thermally stable, cheap, and environmentally benign heterogeneous nanocatalyst that could be reused for many consecutive experiments without significant loss of its activity.

We thank the Shiraz University of Technology and Yasouj University Research Councils for partial support of this work.

Experimental Part

General. All reagents were purchased from either *Fluka* or *Merck*. GO was prepared using a modified *Hummers*' method from flake graphite [28]. *N*-Propargylated nucleobases **1a**–**1h** were prepared according to a modified *Lazrek* and co-workers' method (note: a small amount of TBAB, *i.e.*, 0.1 g, was added for 10 mmol reaction's scale) [25]. Azido alcohols **2a**–**2h** were prepared according to our previously reported method [29]. Solvents were purified and stored over 3-Å molecular sieves. Ultrasonication was performed in a *TECNO-GAZ Tecna 3* ultrasonic bath. M.p.: *Electrothermal IA 9000* melting point apparatus; in open capillary tubes; uncorrected. Thin layer chromatography (TLC): *SILG/UV 254* silica gel plates (SiO_2). Column chromatography (CC): SiO_2 *60* (0.063–0.200 mm, 70–230 mesh ASTM). IR Spectra: *Shimadzu FT-IR-8300* spectrophotometer; $\tilde{\nu}$ in cm^{-1}. ^1H- and ^{13}C-NMR spectra: *Bruker Avance-DPX-250* spectrometer (250 and 62.5 MHz, resp.); δ in ppm rel. to Me_4Si as internal standard, *J* in Hz. GC/MS: *Shimadzu GC/MS-QP 1000-EX* apparatus; in *m/z* (rel. %). Elemental analyses: *PerkinElmer 240-B* microanalyzer. TEM: *Philips CM-10* TEM microscope; at 100 kV. Powder X-ray diffraction (XRD): *Bruker AXS D8 Advance* instrument employing reflection *Bragg–Brentano* geometry with CuK_α radiation. Energy-dispersive analysis of X-ray (EDAX): *PHILIPS XL30* instrument; accelerating voltage, 20 kV.

Synthesis of AC/GO Hybrid. In this method, aminoclay nanostructures were allowed to form on the surface of GO sheets dispersed in H_2O. In a typical procedure, for the preparation of AC/GO hybrid 0.2 g of GO were dispersed in 25 ml H_2O by sonication for 10 min. To the dispersion, 0.84 g (3.62 mmol) of $MgCl_2$ was added followed by dropwise addition of 1.0 ml (5.85 mmol) of 3-(trimethoxysilyl)propan-1-amine. The soln. was stirred for 48 h to form a brown-black slurry, which was dried at 100°. The solid thus obtained was dispersed in H_2O (20 ml) and precipitated from EtOH (30 ml). The precipitate was centrifuged and subsequently dried at 60° to obtain the AC/GO hybrid [30].

Synthesis of the Cu/AC/r-GO Nanohybrid. AC/GO (40 mg) was first dispersed in 4 ml of deionized H_2O by sonication. To this transparent AC/GO suspension, 1 ml of 10 mM $CuSO_4 \cdot 5\ H_2O$ soln. was added followed by dropwise addition of 2 ml of 1M $N_2H_4 \cdot H_2O$ soln. Then, Cu/AC/r-GO nanohybrid was precipitated from EtOH (30 ml). The precipitate was centrifuged and subsequently dried *in vacuo* for 1 d at ambient temp. to obtain the Cu/AC/GO nanohybrid [31].

Synthesis of 1,2,3-Triazolyl Carboacyclic Nucleosides **3a**–**3o**. To a 50-ml round-bottom flask was added a mixture of alkyne (0.01 mol), azido alcohol (0.012 mol), and Cu/AC/r-GO nanohybrid (0.4 g, 0.008 mol-%) in H_2O/THF 1:1 (30 ml). The mixture was stirred at r.t. until TLC monitoring indicated no further progress in the conversion. The catalyst was filtered off and washed with THF, and the filtrate was evaporated *in vacuo* to remove the solvent. The remaining foam was dissolved in $CHCl_3$ (100 ml) and subsequently washed with H_2O (3×100 ml). The org. layer was dried (Na_2SO_4) and evaporated. The crude product was purified by CC (SiO_2) and eluted with proper solvents described below.

*1-{[1-(2-Hydroxycyclohexyl)-1*H*-1,2,3-triazol-4-yl]methyl}pyrimidine-2,4(1*H,*3*H*)-dione* (**3a**). Yield: 2.56 g (88%; CC (SiO_2; AcOEt)). Colorless solid. M.p. 229–230°. IR (KBr): 3233 (br.), 3058*s*, 2930*m*, 1718*s*, 1707*s*, 1657*m*, 1495*s*. ^{1}H-NMR ((D$_6$)DMSO): 11.34 (*s*, NH, exchangeable with D_2O); 8.08 (*s*, H–C(5) of triazol); 7.79 (*d*, *J* = 7.8, H–C(6) of uracil); 5.65 (*d*, *J* = 7.8, H–C(5) of uracil); 5.11–4.94 (*m*, $NCH_2C{=}C$, C*H*OH); 4.24–4.22 (*m*, NCH); 3.75 (*s*, OH, exchangeable with D_2O); 2.02–1.73 (*m*, 4 CH_2). ^{13}C-NMR ((D$_6$)DMSO): 163.59; 150.69; 145.45; 141.46; 122.66; 101.15; 71.16; 65.84; 63.09; 42.31; 34.78; 31.79; 24.53. MS: 291 (16.1, M^+). Anal. calc. for $C_{13}H_{17}N_5O_3$ (291.31): C 53.60, H 5.88, N 24.04; found: C 53.52, H 5.76, N 23.95.

*1-{[1-(2-Hydroxyoctyl)-1*H*-1,2,3-triazol-4-yl]methyl}pyrimidine-2,4(1*H,*3*H*)-dione* (**3b**). Yield: 2.95 g (92%; CC (SiO_2; AcOEt)). Colorless solid. M.p. 146–147°. IR (KBr): 3300 (br.), 3080*s*, 2978*m*, 1720*s*, 1708*s*, 1663*m*, 1475*s*. ^{1}H-NMR ((D$_6$)DMSO): 11.36 (*s*, NH, exchangeable with D_2O); 8.04 (*s*, H–C(5) of triazol); 7.77 (*d*, *J* = 7.7, H–C(6) of uracil); 5.65 (*d*, *J* = 7.7, H–C(5) of uracil); 5.12–5.02 (*m*, C*H*OH); 4.98 (*s*, $NCH_2C{=}C$); 4.42–4.20 (*m*, NCH_2CH); 3.83 (*s*, OH, exchangeable with D_2O); 1.39–1.28 (*m*, 5 CH_2); 0.90 (*t*, *J* = 6.7, Me). ^{13}C-NMR ((D$_6$)DMSO): 163.51; 150.68; 145.40; 141.81; 124.25; 101.13; 68.85; 55.40; 42.23; 34.26; 31.16; 28.58; 24.71; 21.97; 13.87. MS: 321 (12.5, M^+). Anal. calc. for $C_{15}H_{23}N_5O_3$ (321.38): C 56.06, H 7.21, N 21.79; found: C 55.98, H 7.15, N 21.85.

*1-{[1-(2-Hydroxybutyl)-1*H*-1,2,3-triazol-4-yl]methyl}pyrimidine-2,4(1*H,*3*H*)-dione* (**3c**). Yield: 2.38 g (90%; CC (SiO_2; AcOEt)). Colorless solid. M.p. 142–143°. IR (KBr): 3400 (br.), 3028*s*, 2956*m*, 1714*s*, 1701*s*, 1662*m*, 1472*s*. ^{1}H-NMR ((D$_6$)DMSO): 10.07 (*s*, NH, exchangeable with D_2O); 8.11 (*s*, H–C(5) of triazol); 7.66 (*d*, *J* = 7.5, H–C(6) of uracil); 5.92 (*d*, *J* = 7.5, H–C(5) of uracil); 5.52 (*s*, $NCH_2C{=}C$); 4.94–4.97 (*m*, C*H*OH); 4.28 (*dd*, *J* = 13.6, 3.2, 1 H of NCH_2CH); 4.12 (*dd*, *J* = 13.6, 7.4, 1 H of NCH_2CH); 3.68 (*s*, OH, exchangeable with D_2O); 1.35–1.13 (*m*, $MeCH_2$); 0.85 (*t*, *J* = 7.2, *Me*CH_2). ^{13}C-NMR ((D$_6$)DMSO): 163.62; 150.77; 143.28; 141.39; 123.84; 102.86; 71.84; 61.52; 50.21; 28.01; 9.79. MS: 265 (13.8, M^+). Anal. calc. for $C_{11}H_{15}N_5O_3$ (265.27): C 49.81, H 5.70, N 26.40; found: C 49.89, H 5.64, N 26.48.

*1-({1-[3-(4-Chlorophenoxy)-2-hydroxypropyl]-1*H*-1,2,3-triazol-4-yl}methyl)pyrimidine-2,4(1*H,*3*H*)-dione* (**3d**). Yield: 3.17 g (84%; CC (SiO_2; AcOEt)). Colorless solid. M.p. 165–166°. IR (KBr): 3260 (br.), 3035*s*, 2968*m*, 1716*s*, 1704*s*, 1659*m*, 1461*s*, 1210*s*, 768*s*. ^{1}H-NMR ((D$_6$)DMSO): 11.12 (*s*, NH, exchangeable with D_2O); 7.85 (*s*, H–C(5) of triazol); 7.48 (*d*, *J* = 7.5, H–C(6) of uracil); 7.11 (*m*, 2 arom. H); 6.78 (*m*, 2 arom. H); 5.42 (*d*, *J* = 7.5, H–C(5) of uracil); 4.74 (*s*, $NCH_2C{=}C$); 4.40–4.23 (*m*, C*H*OH, CH_2O); 4.01 (*s*, OH, exchangeable with D_2O); 3.77–3.70 (*m*, NCH_2CH). ^{13}C-NMR ((D$_6$)DMSO): 163.71; 157.10; 150.93; 145.40; 141.98; 134.53; 129.16; 124.58; 116.19; 101.19; 69.79; 67.62; 52.58; 42.29. MS: 377 (10.3, M^+). Anal. calc. for $C_{16}H_{16}ClN_5O_4$ (377.78): C 50.87, H 4.27, Cl 9.38, N 18.54; found: C 50.81, H 4.32, Cl 9.46, N 18.48.

*2-({1-[3-(2,4-Dichlorophenoxy)-2-hydroxypropyl]-1*H*-1,2,3-triazol-4-yl}methyl)-1,2,4-triazine-3,5(2*H*,4*H*)-dione* (**3e**). Yield: 3.34 g (81%; CC (SiO_2; AcOEt)). White solid. M.p. 202–203°. IR (KBr): 3345 (br.), 3100*s*, 2971*m*, 1720*s*, 1705*s*, 1663*m*, 1459*s*, 1215*s*, 775*s*. ^{1}H-NMR ((D_6)DMSO): 12.54 (*s*, NH, exchangeable with D_2O); 7.88 (*s*, H–C(5) of triazol); 7.42 (*s*, H–C(5) of azauracil, 1 arom. H); 7.25–7.20 (*m*, 1 arom. H); 7.05 (*d*, J = 7.5, 1 arom. H); 5.50 (*s*, OH, exchangeable with D_2O); 4.87 (*s*, NCH_2C=C); 4.49–4.26 (*m*, C*H*OH, CH_2O); 3.95–3.84 (*m*, NCH_2CH). ^{13}C-NMR ((D_6)DMSO): 155.84; 152.77; 148.81; 141.30; 134.70; 129.20; 128.03; 124.68; 124.55; 122.46; 115.17; 70.64; 67.52; 52.47; 34.40. MS: 413 (15.7, M^+). Anal. calc. for $C_{15}H_{14}Cl_2N_6O_4$ (413.22): C 43.60, H 3.41, Cl 17.16, N 20.34; found: C 43.67, H 3.35, Cl 17.24, N 20.29.

*3,7-Dihydro-7-({1-[2-hydroxy-3-(4-methylphenoxy)propyl]-1*H*-1,2,3-triazol-4-yl}methyl)-1,3-dimethyl-1*H*-purine-2,6-dione* (**3f**). Yield: 3.95 g (93%; CC (SiO_2; AcOEt)). Colorless solid. M.p. 116–117°. IR (KBr): 3250 (br.), 3100*s*, 2945*m*, 1723*s*, 1711*s*, 1657*m*, 1461*s*, 1223*s*. ^{1}H-NMR ((D_6)DMSO): 8.02 (*s*, H–C(8) of theophenyl); 7.97 (*s*, H–C(5) of triazol); 6.91 (*d*, J = 8.2, 2 arom. H); 6.65 (*d*, J = 8.2, 2 arom. H); 5.43 (*s*, NCH_2C=C); 4.61–4.41 (*m*, CH_2O); 4.34–4.25 (*m*, C*H*OH); 4.09 (br. *s*, OH, exchangeable with D_2O); 3.79–3.72 (*m*, NCH_2CH); 3.32 (*s*, Me–N(1)); 3.24 (*s*, Me–N(3)); 2.07 (*s*, Ar–Me). ^{13}C-NMR ((D_6)DMSO): 162.23; 156.08; 154.30; 150.83; 148.15; 134.47; 133.00; 129.37; 124.76; 114.15; 105.70; 69.36; 67.73; 52.67; 41.02; 29.25; 27.39; 19.92. MS: 425 (9.5, M^+). Anal. calc. for $C_{20}H_{23}N_7O_4$ (425.45): C 56.46, H 5.45, N 23.05; found: C 56.40, H 5.41, N 23.14.

*3,7-Dihydro-7-({1-[2-hydroxy-3-(4-methoxyphenoxy)propyl]-1*H*-1,2,3-triazol-4-yl}methyl)-1,3-dimethyl-1*H*-purine-2,6-dione* (**3g**). Yield: 3.97 g (90%; CC (SiO_2; AcOEt)). Colorless solid. M.p. 183–184°. IR (KBr): 3222 (br.), 3127*s*, 2931*m*, 1725*s*, 1710*s*, 1657*m*, 1439*s*, 1236*s*. ^{1}H-NMR ((D_6)DMSO): 8.13 (*s*, H–C(8) of theophenyl); 8.07 (*s*, H–C(5) of triazol); 6.83–6.75 (*m*, 4 arom. H); 5.54 (*s*, NCH_2C=C); 5.51–5.49 (*m*, C*H*OH); 4.51 (*dd*, J = 13.8, 3.3, 1 H of CH_2O); 4.35 (*dd*, J = 13.8, 7.5, 1 H of CH_2O); 4.15 (*s*, OH, exchangeable with D_2O); 3.83–3.80 (*m*, NCH_2CH); 3.65 (*s*, MeO); 3.35 (*s*, Me–N(1)); 3.16 (*s*, Me–N(3)). ^{13}C-NMR ((D_6)DMSO): 154.29; 153.43; 152.22; 150.85; 148.17; 142.27; 141.99; 124.77; 115.31; 114.40; 105.72; 69.96; 67.75; 55.21; 52.68; 41.04; 29.28; 27.42. MS: 441 (10.3, M^+). Anal. calc. for $C_{20}H_{23}N_7O_5$ (441.45): C 54.42, H 5.25, N 22.21; found: C 54.31, H 5.39, N 22.27.

*3,7-Dihydro-7-{[1-(2-hydroxyethyl)-1*H*-1,2,3-triazol-4-yl]methyl}-1,3-dimethyl-1*H*-purine-2,6-dione* (**3h**). Yield: 2.86 g (94%; CC (SiO_2; AcOEt/hexane 10:1)). Colorless solid. M.p. 186–187°. IR (KBr): 3248 (br.), 3064*s*, 2952*m*, 1718*s*, 1706*s*, 1668*m*, 1449*s*. ^{1}H-NMR ($CDCl_3$): 8.19 (*s*, H–C(8) of theophenyl); 8.09 (*s*, H–C(5) of triazol); 5.59 (*s*, NCH_2C=C); 4.38 (*t*, J = 5.2, CH_2O); 3.77 (*t*, J = 5.2, NCH_2CH_2); 3.43 (*s*, Me–N(1)); 3.39 (*s*, OH, exchangeable with D_2O); 3.24 (*s*, Me–N(3)). ^{13}C-NMR ($CDCl_3$): 159.23; 154.41; 152.16; 148.63; 143.15; 122.54; 108.09; 63.37; 56.51; 49.53; 33.48; 29.88. MS: 305 (11.6, M^+). Anal. calc. for $C_{12}H_{15}N_7O_3$ (305.30): C 47.21, H 4.95, N 32.12; found: C 47.34, H 5.03, N 32.08.

*3,7-Dihydro-1-{[1-(2-hydroxyethyl)-1*H*-1,2,3-triazol-4-yl]methyl}-3,7-dimethyl-1*H*-purine-2,6-dione* (**3i**). Yield: 2.44 g (80%; CC (SiO_2; AcOEt/MeOH 7:1)). Colorless solid. M.p. 212–213°. IR (KBr): 3300 (br.), 3058*s*, 2947*m*, 1720*s*, 1708*s*, 1661*m*, 1469*s*. ^{1}H-NMR ((D_6)DMSO): 8.04 (*s*, H–C(8) of theobromin); 7.94 (*s*, H–C(5) of triazol); 5.12 (*s*, NCH_2C=C); 5.05 (*s*, OH, exchangeable with D_2O); 4.35 (*t*, J = 5.2, CH_2O); 3.90 (*s*, Me–N(7)); 3.76 (*t*, J = 5.2, NCH_2CH_2); 3.43 (*s*, Me–N(3)). ^{13}C-NMR ((D_6)DMSO): 155.29; 151.72; 150.80; 146.02; 143.58; 123.59; 106.59; 58.78; 56.39; 43.52; 31.28; 30.68. MS: 305 (14.9, M^+). Anal. calc. for $C_{12}H_{15}N_7O_3$ (305.30): C 47.21, H 4.95, N 32.12; found: C 47.31, H 4.90, N 32.17.

*2-{4-[(6-Amino-9*H*-purin-9-yl)methyl]-1*H*-1,2,3-triazol-1-yl}ethanol* (**3j**). Yield: 2.13 g (82%; CC (SiO_2; AcOEt/MeOH 1:4)). Gray solid. M.p. >280° (dec.). IR (KBr): 3310 (br.), 3075*s*, 2981*m*, 1667*m*, 1458*s*. ^{1}H-NMR ((D_6)DMSO): 8.18 (*s*, H–C(8) of adenine); 7.91 (*s*, H–C(5) of triazol); 7.78 (*s*, H–C(2) of adenine); 7.21 (*s*, NH_2, exchangeable with D_2O); 4.65 (*s*, NCH_2C=C); 4.34 (*t*, J = 7.0, CH_2O); 4.16 (*s*, OH, exchangeable with D_2O); 3.78 (*t*, J = 7.0, NCH_2CH_2). ^{13}C-NMR ((D_6)DMSO): 160.82; 153.63; 149.75; 144.96; 141.95; 124.60; 120.73; 60.87; 59.68; 58.49. MS: 260 (17.4, M^+). Anal. calc. for $C_{10}H_{12}N_8O$ (260.26): C 46.15, H 4.65, N 43.06; found: C 46.21, H 4.74, N 43.15.

*3-{4-[(6-Amino-9*H*-purin-9-yl)methyl]-1*H*-1,2,3-triazol-1-yl}propan-1-ol* (**3k**). Yield: 2.33 g (85%; CC (SiO_2; AcOEt/MeOH 1:4)). Gray solid. M.p. >310° (dec.). IR (KBr): 3300 (br.), 3040*s*, 2973*m*, 1665*m*, 1462*s*. ^{1}H-NMR ((D_6)DMSO): 8.25 (*s*, H–C(8) of adenine); 8.22 (*s*, H–C(5) of triazol); 8.12 (*s*, H–C(2) of adenine); 7.32 (*s*, NH_2, exchangeable with D_2O); 4.96 (*s*, NCH_2C=C); 4.62 (*s*, OH,

exchangeable with D_2O); 4.23 (*t*, *J* = 7.7, CH_2O); 3.85 (*t*, *J* = 7.7, NCH_2CH_2); 1.90–1.78 (*m*, NCH_2CH_2). ^{13}C-NMR ((D_6)DMSO): 160.57; 154.24; 148.76; 145.01; 141.88; 125.09; 121.64; 63.94; 59.92; 50.69; 33.10. MS: 274 (9.7, M^+). Anal. calc. for $C_{11}H_{14}N_8O$ (274.29): C 48.17, H 5.14, N 40.85; found: C 48.25, H 5.06, N 40.80.

*2-[4-(1*H*-Benzimidazol-1-ylmethyl)-1*H*-1,2,3-triazol-1-yl]ethanol* (**3l**). Yield: 2.09 g (86%; CC (SiO_2; AcOEt)). Colorless solid. M.p. 150–151°. IR (KBr): 3237 (br.), 3046*s*, 2983*m*, 1670*m*, 1476*s*. ^{1}H-NMR ((D_6)DMSO): 8.33 (*s*, H–C(2) of benzimidazole); 8.12 (*s*, H–C(5) of triazol); 7.68–7.63 (*m*, 2 arom. H); 7.27–7.16 (*m*, 2 arom. H); 5.56 (*s*, $NCH_2C{=}C$); 4.34 (*t*, *J* = 5.2, CH_2O); 3.70 (*t*, *J* = 5.2, NCH_2CH_2); 3.40 (*s*, OH, exchangeable with D_2O). ^{13}C-NMR ((D_6)DMSO): 145.65; 144.52; 141.17; 135.33; 126.98; 124.76; 123.35; 117.24; 116.10; 59.30; 57.37; 55.70. MS: 243 (9.2, M^+). Anal. calc. for $C_{12}H_{13}N_5O$ (243.27): C 59.25, H 5.39, N 28.79; found: C 59.37, H 5.31, N 28.84.

*1-[4-(1*H*-Benzimidazol-1-ylmethyl)-1*H*-1,2,3-triazol-1-yl]-3-phenoxypropan-2-ol* (**3m**). Yield: 2.79 g (80%; CC (SiO_2; AcOEt)). Yellow oil. IR (film): 3283 (br.), 3052*s*, 2960*m*, 1671*m*, 1457*s*, 1225*s*. ^{1}H-NMR ((D_6)DMSO): 8.18 (*s*, H–C(2) of benzimidazole); 8.08 (*s*, H–C(5) of triazol); 7.33–7.04 (*m*, 9 arom. H); 5.59–5.57 (*m*, C*H*OH); 5.13 (*s*, $NCH_2C{=}C$); 4.56 (*dd*, *J* = 13.8, 3.4, 1 H of CH_2O); 4.39 (*dd*, *J* = 13.8, 7.6, 1 H of CH_2O); 4.21 (*s*, OH, exchangeable with D_2O); 3.90–3.85 (*m*, NCH_2CH). ^{13}C-NMR ((D_6)DMSO): 159.15; 146.08; 143.81; 139.68; 135.22; 130.11; 124.68; 123.42; 122.12; 120.51; 118.61; 116.35; 114.78; 73.31; 65.91; 61.46; 59.84. MS: 349 (8.5, M^+). Anal. calc. for $C_{19}H_{19}N_5O_2$ (349.39): C 65.32, H 5.48, N 20.04; found: C 65.37, H 5.46, N 20.10.

*2-[4-[(2-Methyl-1*H*-benzimidazol-1-yl)methyl]-1*H*-1,2,3-triazol-1-yl}ethanol* (**3n**). Yield: 2.23 g (87%; CC (SiO_2; AcOEt)). Creamy solid. M.p. 170–171°. IR (KBr): 3320 (br.), 3080*s*, 2945*m*, 1668*m*, 1481*s*. ^{1}H-NMR ((D_6)DMSO): 8.05 (*s*, H–C(5) of triazol); 7.25–7.09 (*m*, 4 arom. H); 4.65 (*s*, $NCH_2C{=}C$); 4.40 (*t*, *J* = 7.2, CH_2O); 4.06 (*s*, OH, exchangeable with D_2O); 3.74 (*t*, *J* = 7.2, NCH_2CH_2); 2.48 (*s*, Me). ^{13}C-NMR ((D_6)DMSO): 147.33; 144.90; 141.87; 135.46; 127.51; 125.08; 123.54; 118.69; 117.16; 60.12; 59.20; 57.68; 18.02. MS: 257 (15.1, M^+). Anal. calc. for $C_{13}H_{15}N_5O$ (257.30): C 60.69, H 5.88, N 27.22; found: C 60.62, H 5.31, N 27.29.

*3-[4-[(2-Methyl-4-nitro-1*H*-imidazol-1-yl)methyl]-1*H*-1,2,3-triazol-1-yl}propan-1-ol* (**3o**). Yield: 2.42 g (91%; CC (SiO_2; AcOEt)). Brown oil. IR (film): 3325 (br.), 3050*s*, 2972*m*, 1665*m*, 1537*s*, 1486*s*, 1348*s*. ^{1}H-NMR ((D_6)DMSO): 8.01 (*s*, H–C(5) of triazol); 7.82 (*s*, H–C(5) of imidazole); 4.83 (*s*, $NCH_2C{=}C$); 4.17 (*s*, OH, exchangeable with D_2O); 3.83–3.78 (*m*, CH_2O, NCH_2CH_2); 2.47 (*s*, Me); 1.94–1.89 (*m*, NCH_2CH_2). ^{13}C-NMR ((D_6)DMSO): 152.99; 148.88; 144.83; 124.16; 119.46; 61.52; 52.13; 47.78; 29.89; 15.79. MS: 266 (10.7, M^+). Anal. calc. for $C_{10}H_{14}N_6O_3$ (266.26): C 45.11, H 5.30, N 31.56; found: C 45.17, H 5.38, N 31.49.

REFERENCES

[1] 'Modified Nucleosides: in Biochemistry, Biotechnology and Medicine', Ed. P. Herdewijn, Wiley-VCH, Weinheim, 2008.

[2] 'Chemical Synthesis of Nucleoside Analogues', Ed. P. Merino, John Wiley & Sons, Inc., Hoboken, 2013.

[3] F. de Carvalho da Silva, M. F. do Carmo Cardoso, P. Garcia Ferreira, V. F. Ferreira, *Top. Heterocycl. Chem.* **2015**, *40*, 117.

[4] E. De Clercq, *Clin. Microbiol. Rev.* **1997**, *10*, 674; E. De Clercq, *Nat. Rev. Drug Discovery* **2002**, *1*, 13; R. Alvarez, S. Velazquez, A. San-Felix, S. Aquaro, E. De Clercq, C.-F. Perno, A. Karlsson, J. Balzarini, M. J. Camarasa, *J. Med. Chem.* **1994**, *37*, 4185; H. Ishikawa, *Curr. Med. Chem.* **1999**, *6*, 575.

[5] E. De Clercq, *J. Clin. Virol.* **2004**, *30*, 115.

[6] D. Baraniak, K. Kacprzak, L. Celewicz, *Bioorg. Med. Chem. Lett.* **2011**, *21*, 723; H. Ding, R. Yang, Y. Song, Q. Xiao, J. Wu, *Nucleosides, Nucleotides Nucleic Acids* **2008**, *27*, 368.

[7] F. Amblard, J. H. Cho, R. F. Schinazi, *Chem. Rev. (Washington, DC, U.S.)* **2009**, *109*, 4207.

[8] J. E. Moses, A. D. Moorhouse, *Chem. Soc. Rev.* **2007**, *36*, 1249.

[9] M. Koszytkowska-Stawińska, E. Mironiuk-Puchalska, T. Rowicki, *Tetrahedron* **2012**, *68*, 214, and references cited therein.

[10] 'Click Chemistry for Biotechnology and Materials Science', Ed. J. Lahann, John Wiley & Sons, Ltd., Chichester, 2009.
[11] Q. Wang, S. Chittaboina, H. N. Barnhill, *Lett. Org. Chem.* **2005**, *2*, 293.
[12] F. Himo, T. Lovell, R. Hilgraf, V. V. Rostovtsev, L. Noodleman, K. B. Sharpless, V. V. Fokin, *J. Am. Chem. Soc.* **2005**, *127*, 210.
[13] S. Quader, S. E. Boyd, I. D. Jenkins, T. A. Houston, *J. Org. Chem.* **2007**, *72*, 1962.
[14] P. Siemsen, R. C. Livingston, F. Diederich, *Angew. Chem., Int. Ed.* **2000**, *39*, 2632.
[15] B. Gerard, J. Ryan, A. B. Beeler, J. A. Porco Jr., *Tetrahedron* **2006**, *62*, 6405.
[16] M. N. Soltani Rad, S. Behrouz, M. M. Doroodmand, A. Movahedian, *Tetrahedron* **2012**, *68*, 7812, and references cited therein.
[17] T. Miao, L. Wang, *Synthesis* **2008**, 363; C. Girard, E. Önen, M. Aufort, S. Beauvière, E. Samson, J. Herscovici, *Org. Lett.* **2006**, *8*, 1689.
[18] S. Mao, H. Pu, J. Chen, *RSC Adv.* **2012**, *2*, 2643.
[19] D. Chen, H. Feng, J. Li, *Chem. Rev. (Washington, DC, U.S.)* **2012**, *112*, 6027; I. V. Lightcap, P. V. Kamat, *Acc. Chem. Res.* **2013**, *46*, 2235; C. Chung, Y.-K. Kim, D. Shin, S.-R. Ryoo, B. H. Hong, D.-H. Min, *Acc. Chem. Res.* **2013**, *46*, 2211.
[20] C. K. Chua, M. Pumera, *Chem. Soc. Rev.* **2014**, *43*, 291.
[21] M. N. Soltani Rad, S. Behrouz, A. Movahedian, M. M. Doroodmand, Y. Ghasemi, S. Rasoul-Amini, A.-R. Ahmadi Gandomani, R. Rezaie, *Helv. Chim. Acta* **2013**, *96*, 688.
[22] Y. Si, E. T. Samulski, *Chem. Mater.* **2008**, *20*, 6792.
[23] A. J. Patil, E. Muthusamy, S. Mann, *Angew. Chem., Int. Ed.* **2004**, *43*, 4928.
[24] H. A. Becerril, J. Mao, Z. Liu, R. M. Stoltenberg, Z. Bao, Y. Chen, *ACS Nano* **2008**, *2*, 463.
[25] H. B. Lazrek, M. Taourirte, T. Oulih, M. Lebtoumi, J. L. Barascut, J. L. Imbach, *Nucleosides Nucleotides* **1997**, *16*, 1115.
[26] http://en.wikipedia.org/wiki/Discovery_and_development_of_nucleoside_and_nucleotide_reverse-transcriptase_inhibitors (access date June 15, 2015).
[27] C. R. Martinez, B. L. Iverson, *Chem. Sci.* **2012**, *3*, 2191; C. A. Hunter, J. K. M. Sanders, *J. Am. Chem. Soc.* **1990**, *112*, 5525; M. O. Sinnokrot, C. D. Sherrill, *J. Am. Chem. Soc.* **2004**, *126*, 7690.
[28] W. S. Hummers Jr., R. E. Offeman, *J. Am. Chem. Soc.* **1958**, *80*, 1339; S. J. Hoseini, M. Dehghani, H. Nasrabadi, *Catal. Sci. Technol.* **2014**, *4*, 1078.
[29] M. N. Soltani Rad, S. Behrouz, F. Karimitabar, A. Khalafi-Nezhad, *Helv. Chim. Acta* **2012**, *95*, 491.
[30] A. Achari, K. K. R. Datta, M. De, V. P. Dravid, M. Eswaramoorthy, *Nanoscale* **2013**, *5*, 5316.
[31] K. K. R. Datta, C. Kulkarni, M. Eswaramoorthy, *Chem. Commun.* **2010**, *46*, 616.

Received June 14, 2015